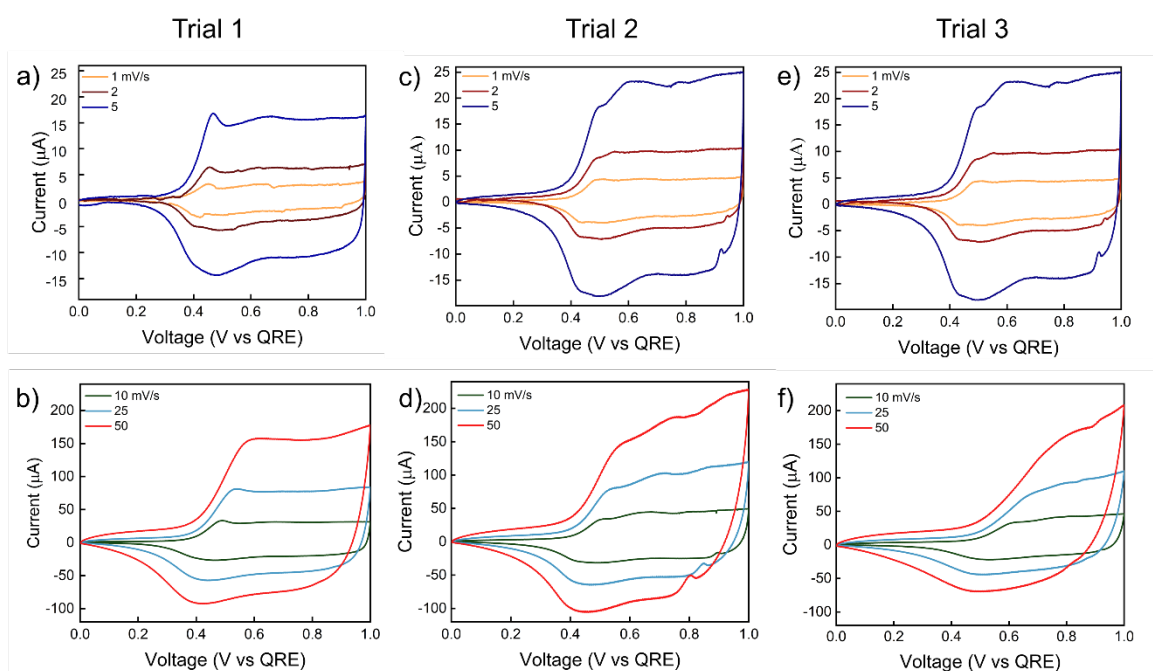


## Electronic Supplementary Information

Real time quantification of mixed ion and electron transfer associated with the doping of poly(3-hexylthiophene)

Ratul M. Thakur,<sup>a</sup> Alexandra D. Easley,<sup>b</sup> Shaoyang Wang,<sup>a</sup> Yiren Zhang,<sup>c</sup> Christopher K. Ober,<sup>c</sup> Jodie L. Lutkenhaus.\*<sup>ab</sup>

- Artie McFerrin Department of Chemical Engineering, Texas A&M University, College Station, Texas 77840, USA
- Department of Materials Science and Engineering, Texas A&M University, College Station, Texas 77840, USA
- Materials Science and Engineering, Cornell University, Ithaca, New York, USA.



**Figure S1.** CVs for three separate P3HT films: Trial 1 (a, b); Trial 2 (c-d); and Trial 3 (e, f). (a, c, e) Scan rates of 1, 2, and 5 mV/s. (b, d, and f). Scan rates of 10, 25, and 50 mV/s.

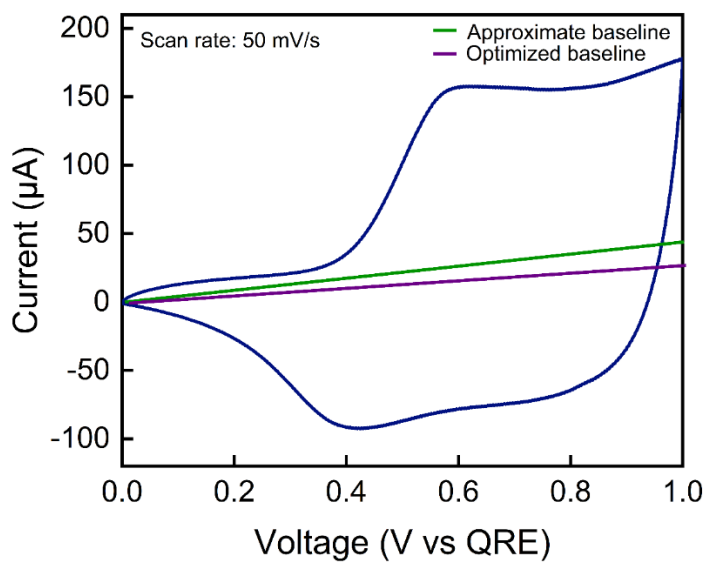
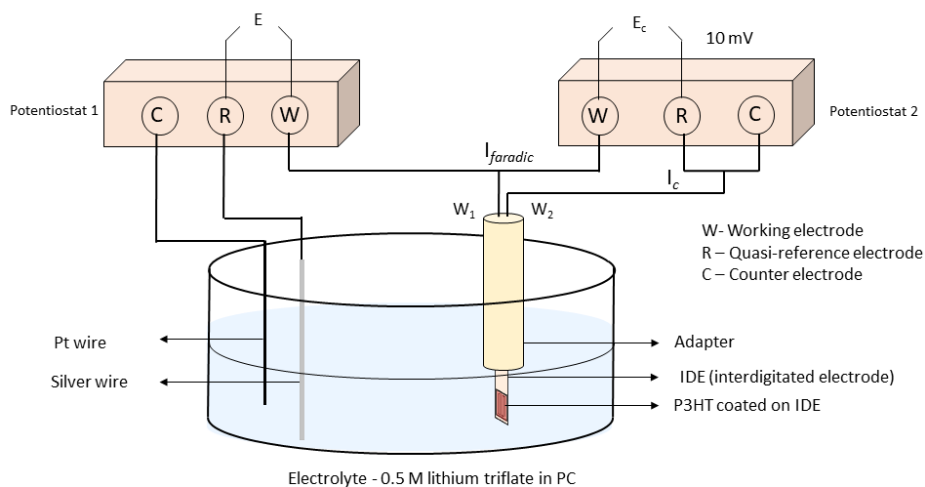


**Figure S2.** Demonstration of equal area baseline methodology to divide the cyclic voltammogram into the oxidation and reduction halves for further analysis. A scan rate of 50 mV/s is shown here.



**Scheme S1.** In-situ conductance setup consisting of two separate potentiostats. P3HT coated on an interdigitated array electrode (IDE) serves as the working electrode. The adapter is connected separately to two different potentiostats (1 and 2). Potentiostat 1 performs cyclic voltammetry using a platinum wire as the counter electrode and silver wire as a quasi-reference electrode. Meanwhile, Potentiostat 2 applies a constant potential bias of  $E_c = 10$  mV across two channels on that same IDE, and the drain current ( $I_c$ ) is measured.  $I_c$  is divided by  $E_c$  to obtain the conductance of the P3HT in real-time.

**Table S1.** Absolute  $\Delta m/Q$  for the different regions and for different scan rates during oxidation and reduction of P3HT taken from **Figure S3 & S4**.

Scan Rate (mV/s)	$\Delta m/Q$ (mg/C)				
	Oxidation			Reduction	
	FI	FII	FIII	RIV	RV
1	$-0.07 \pm 0.31$	$6.44 \pm 0.81$	$3.10 \pm 0.51$	$-3.61 \pm 0.38$	$-2.45 \pm 0.49$
2	$-0.32 \pm 0.01$	$6.61 \pm 0.38$	$2.99 \pm 0.36$	$-3.48 \pm 0.21$	$-3.57 \pm 1.57$
5	$-0.49 \pm 0.23$	$7.03 \pm 0.88$	$2.96 \pm 0.13$	$-3.56 \pm 0.08$	$-2.27 \pm 0.95$
10	$-0.61 \pm 0.14$	$9.48 \pm 1.51$	$3.18 \pm 0.04$	$-3.82 \pm 0.23$	$-2.27 \pm 0.51$
25	$-0.07 \pm 0.87$	$10.59 \pm 0.31$	$3.44 \pm 0.28$	$-3.95 \pm 0.24$	$-2.45 \pm 0.32$
50	$-0.78 \pm 0.27$	$9.27 \pm 1.71$	$3.83 \pm 0.53$	$-4.41 \pm 0.71$	$-3.68 \pm 0.46$

**Table S2.** Apparent molecular weight of transferring species and the number of solvent molecules transferred per ion for the different regions for different scan rates during oxidation and reduction.

<sup>a a</sup>. The moles of solvent incoming were not calculated for FI due to presence of small negative slope.

Scan Rate (mV/s)	Apparent molecular wt (g/mol)					Number of solvent molecules per anion				
	Oxidation			Reduction		Oxidation			Reduction	
	FI	FII	FIII	RIV	RV	FI <sup>a</sup>	FII	FIII	RIV	RV
1	-7.1 ± 3.5	621 ± 77	299 ± 49	-348 ± 37	-237 ± 47	-	4.6 ± 0.8	1.5 ± 0.5	1.9 ± 0.4	0.9 ± 0.5
2	-31.1 ± 1.1	638 ± 67	288 ± 35	-336 ± 21	-344 ± 41	-	4.8 ± 0.6	1.5 ± 0.4	1.8 ± 0.2	1.9 ± 1.5
5	-47.9 ± 22.3	677 ± 85	285 ± 12	-344 ± 8	-219 ± 12	-	5.1 ± 0.8	1.4 ± 0.1	1.9 ± 0.1	0.7 ± 0.9
10	-58.9 ± 13.5	914 ± 146	307 ± 5	-369 ± 22	-219 ± 5	-	7.5 ± 1.4	1.6 ± 0.1	2.2 ± 0.2	0.7 ± 0.5
25	-6.7 ± 84.2	1022 ± 29	331 ± 27	-381 ± 23	-236 ± 27	-	8.5 ± 0.3	1.8 ± 0.3	2.3 ± 0.2	0.9 ± 0.3
50	-75.9 ± 26.7	894 ± 164	370 ± 51	-425 ± 69	-355 ± 44	-	7.3 ± 1.6	2.2 ± 0.5	2.7 ± 0.7	2.1 ± 0.4

<sup>a a</sup>. The moles of solvent incoming were not calculated for FI due to presence of small negative apparent molecular weight.

**Table S3.** Summary of transition voltages with varying cyclic voltammetry scan rates.

	Transition voltage (V vs QRE)		
Scan Rate (mV/s)	Oxidation		Reduction
	FI-FII	FII-FIII	RIV - RV
1	0.28 ± 0.04	0.57 ± 0.05	0.41 ± 0.04
2	0.34 ± 0.03	0.56 ± 0.06	0.41 ± 0.04
5	0.33 ± 0.07	0.55 ± 0.07	0.37 ± 0.04
10	0.31 ± 0.01	0.56 ± 0.05	0.4 ± 0.02
25	0.35 ± 0.07	0.58 ± 0.07	0.36 ± 0.01
50	0.39 ± 0.08	0.61 ± 0.08	0.32 ± 0.01

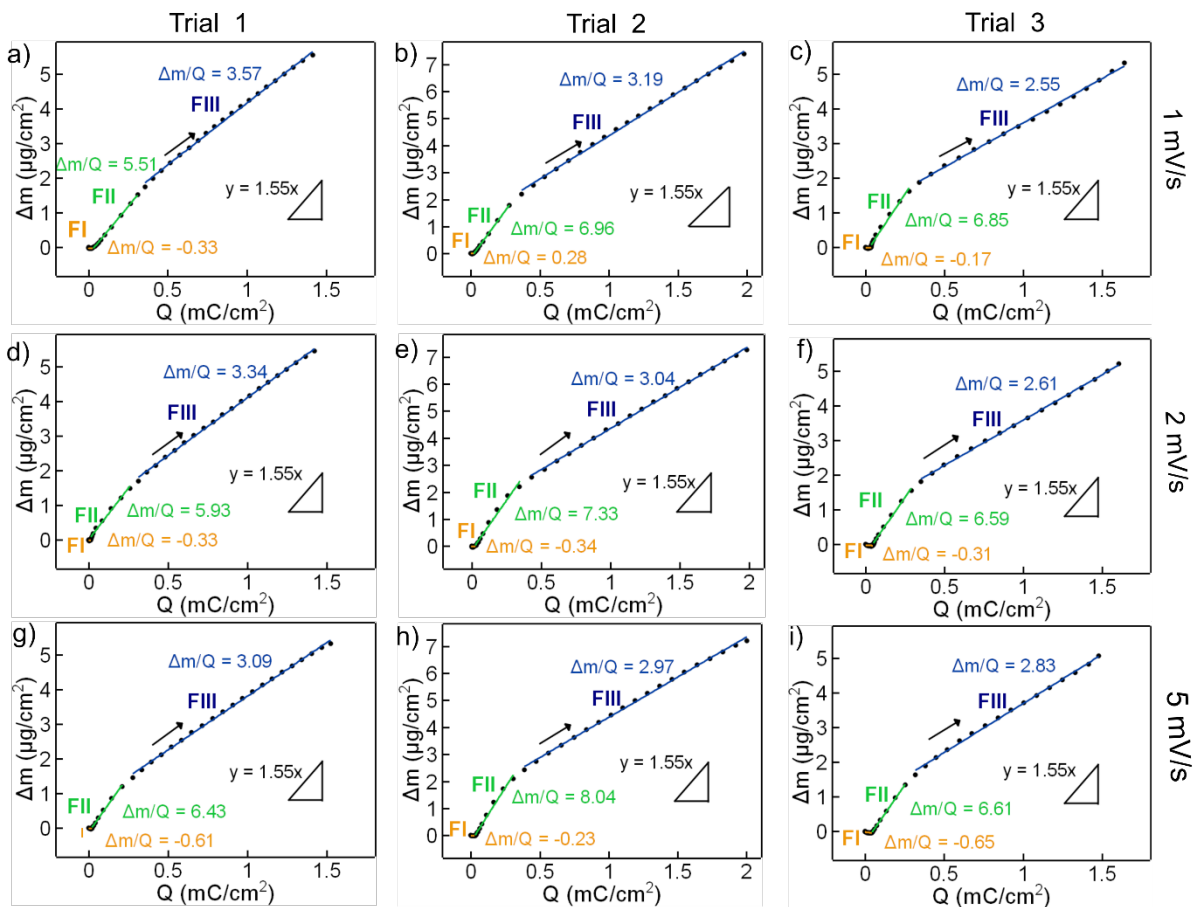


**Figure S3.**  $\Delta m$  vs  $Q$  for the scan rates of 1, 2, and 5 mV/s for three separate P3HT films during the CV oxidation cycle with QCM-D.

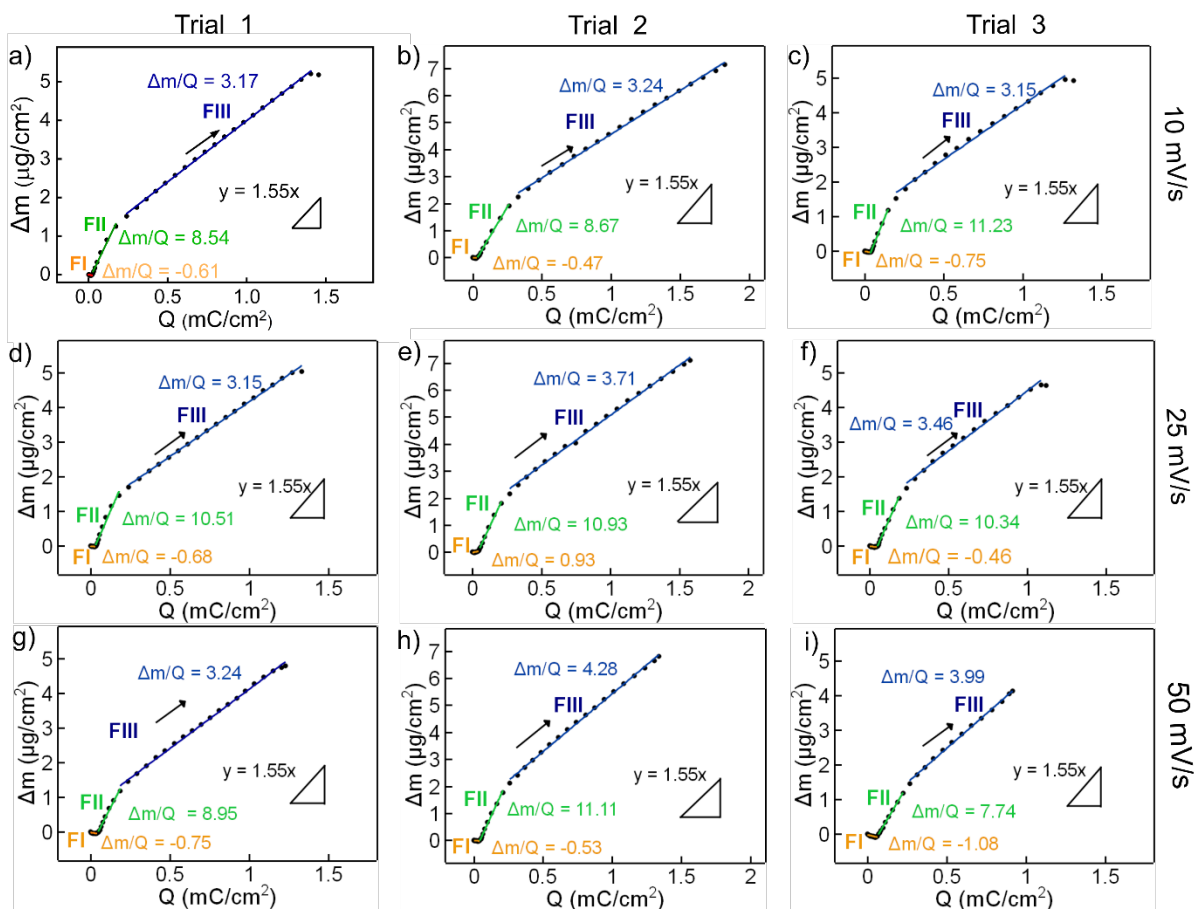


**Figure S4.**  $\Delta m$  vs  $Q$  for the scan rates of 10, 25, and 50 mV/s for three separate P3HT films during the CV oxidation cycle with QCM-D.



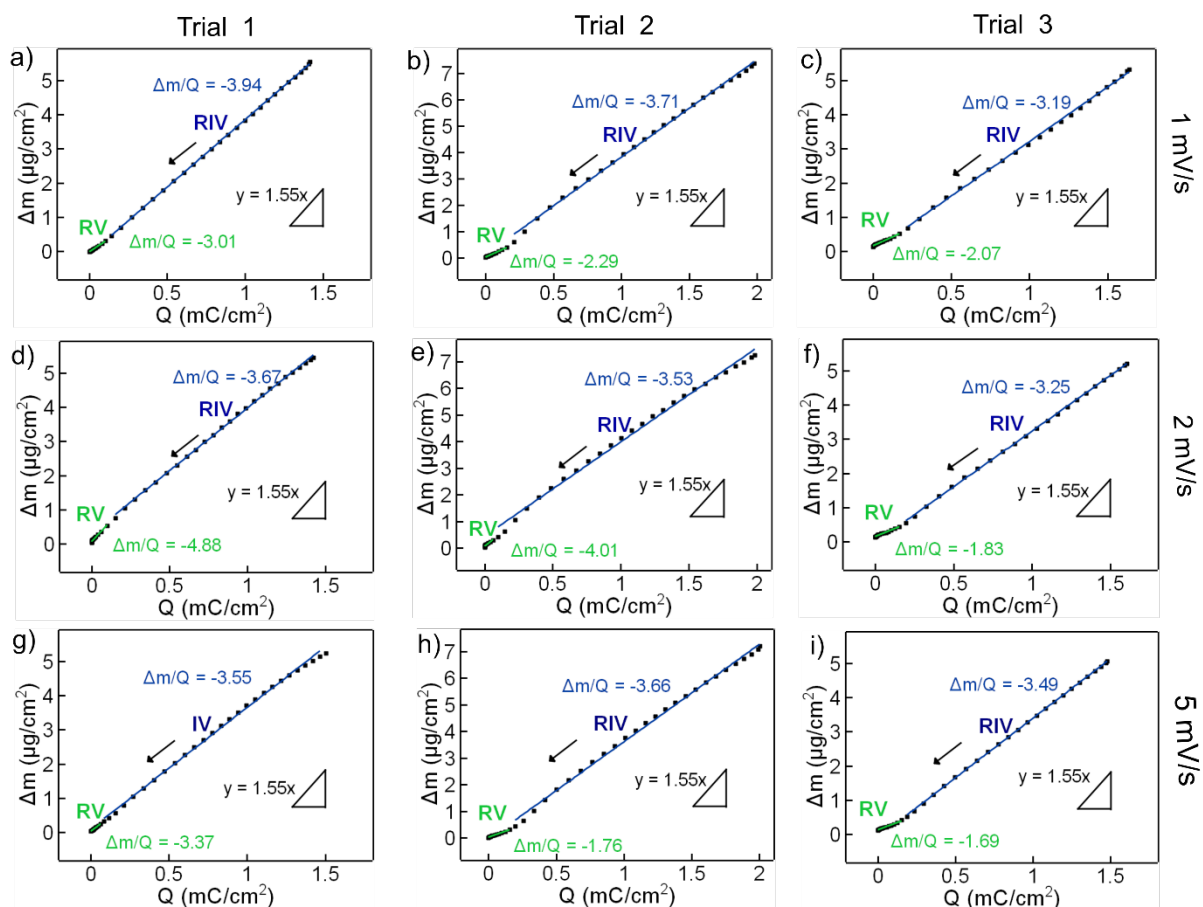


**Figure S5.**  $\Delta m$  vs  $Q$  for the scan rates of 1, 2, and 5 mV/s for three separate P3HT films during the CV reduction cycle with QCM-D.

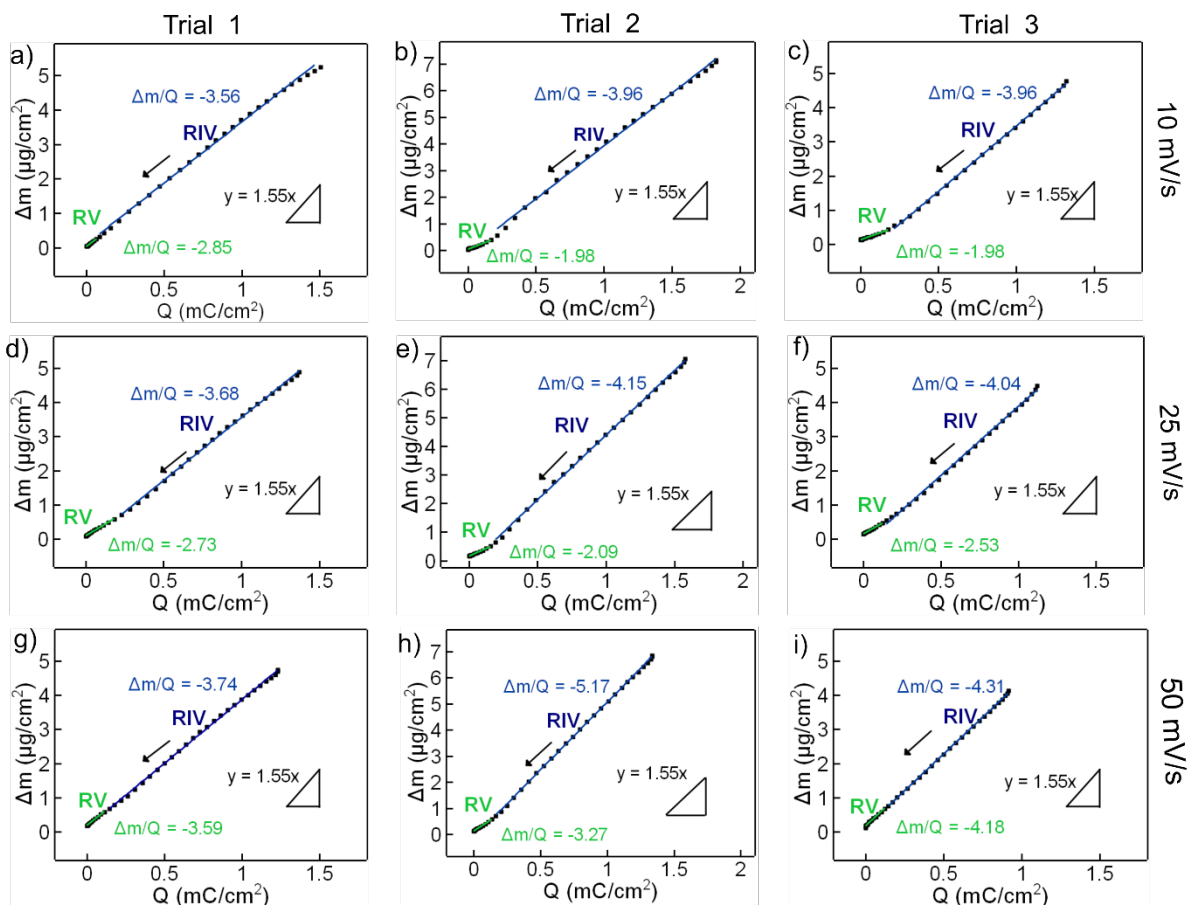


**Figure S6.**  $\Delta m$  vs  $Q$  for the scan rates of 10, 25, and 50 mV/s for three separate P3HT films during the CV reduction cycle with QCM-D.

**Table S4.** Summary of transition voltages with varying galvanostatic charge-discharge C- rates. Only oxidation is described because no distinguishable transitions were observed for reduction.

	Transition voltage (V vs QRE)
C- Rate ( $\text{h}^{-1}$ )	Oxidation
	FI-FII
5	$0.61 \pm 0.06$
10	$0.63 \pm 0.09$
20	$0.69 \pm 0.11$

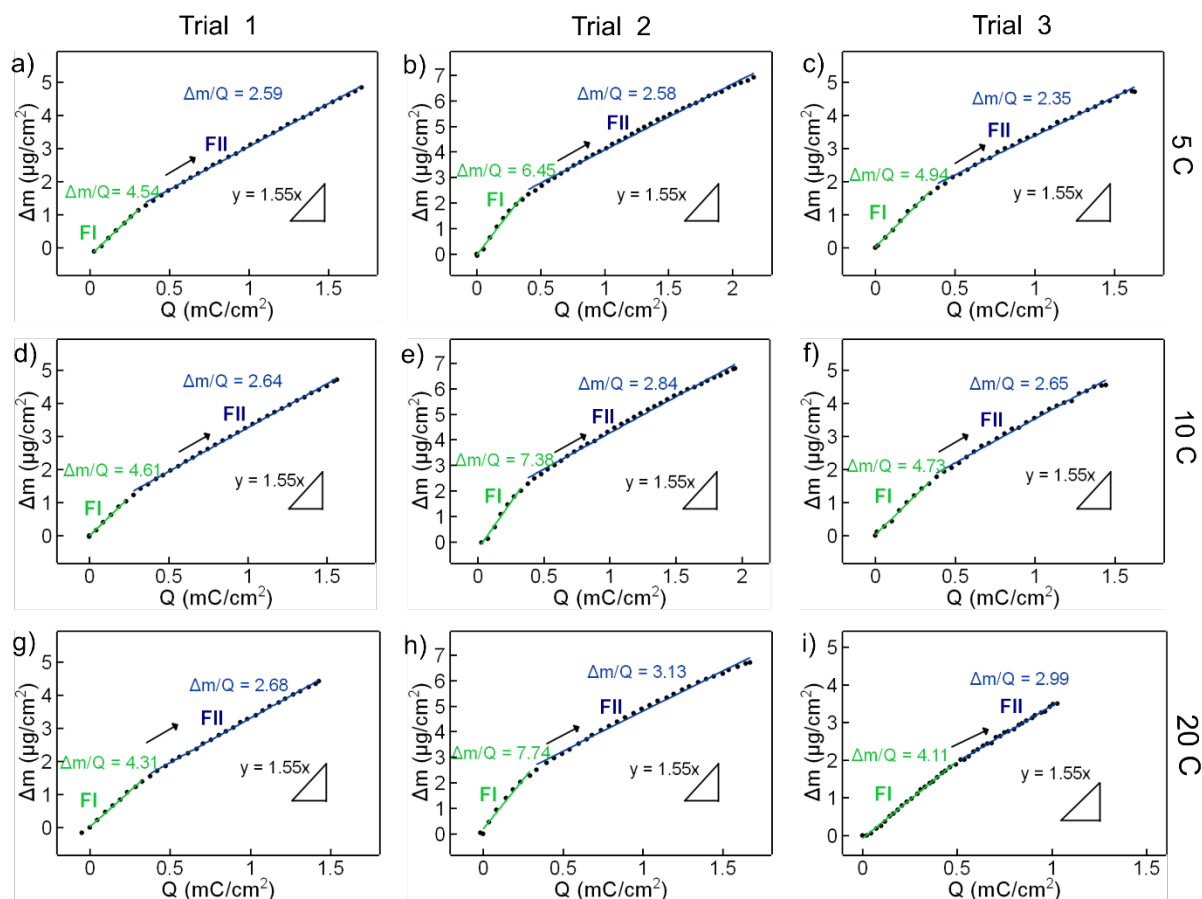


**Figure S7.**  $\Delta m$  vs  $Q$  for three separate P3HT films during the oxidation cycle of GCD with QCM-D at C-rates of 5, 10, and 20.

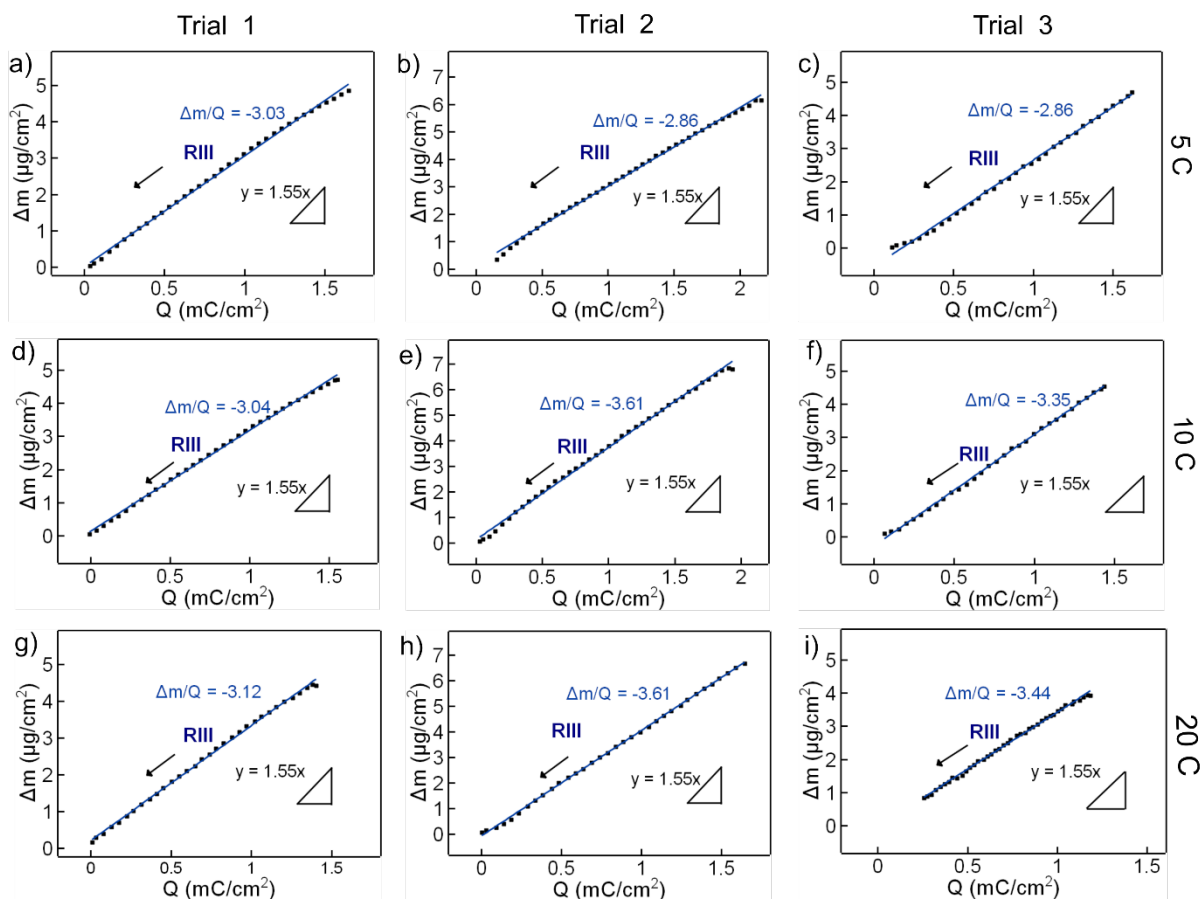


**Figure S8.**  $\Delta m$  vs  $Q$  for three separate P3HT films during the reduction cycle of GCD with QCM-D at C-rates of 5, 10, and 20.

**Table S5.**  $\Delta m/Q$  for the different regions and for different C-rates during oxidation and reduction of P3HT. C- Rate( $h^{-1}$ )

	Absolute $\Delta m/Q$ (mg/C)		
	Oxidation		Reduction
	FI	FII	RIII
5	$5.31 \pm 1.01$	$2.51 \pm 0.13$	$-2.91 \pm 0.38$
10	$5.57 \pm 1.56$	$2.71 \pm 0.11$	$-3.34 \pm 0.21$
20	$5.38 \pm 2.04$	$2.93 \pm 0.23$	$-3.56 \pm 0.08$

**Table S6.** Apparent molecular weight of transporting species and the number of solvent molecules transported per anion for the different regions for different C-rates during oxidation and reduction in GCD.

C- Rate ( $h^{-1}$ )	Apparent molecular wt (g/mol)			Number of solvent molecules per anion		
	Oxidation		Reduction	Oxidation		Reduction
	FI	FII	RIII	FI	FII	RIII
5	$512 \pm 97$	$242 \pm 13$	$-281 \pm 9$	$3.6 \pm 0.9$	$0.9 \pm 0.1$	$1.3 \pm 0.1$
10	$537 \pm 151$	$261 \pm 10$	$-322 \pm 26$	$3.8 \pm 1.5$	$1.1 \pm 0.1$	$1.6 \pm 0.2$
20	$519 \pm 196$	$283 \pm 22$	$-324 \pm 23$	$3.7 \pm 1.9$	$1.3 \pm 0.2$	$1.7 \pm 0.2$

**Table S7.** Summary of transition doping percentages with varying cyclic voltammetry scan rates.

	Transition values for doping regions (%)		
Scan Rate (mV/s)	Oxidation		Reduction
	FI-FII	FII-FIII	RIV - RV
1	0.33 ± 0.02	3.04 ± 0.09	1.42 ± 0.26
2	0.29 ± 0.15	2.86 ± 0.19	1.51 ± 0.28
5	0.29 ± 0.12	2.53 ± 0.23	1.68 ± 0.33
10	0.29 ± 0.12	2.31 ± 0.23	2.01 ± 0.22
25	0.39 ± 0.09	1.88 ± 0.21	1.98 ± 0.13
50	0.41 ± 0.03	1.92 ± 0.31	2.11 ± 0.39

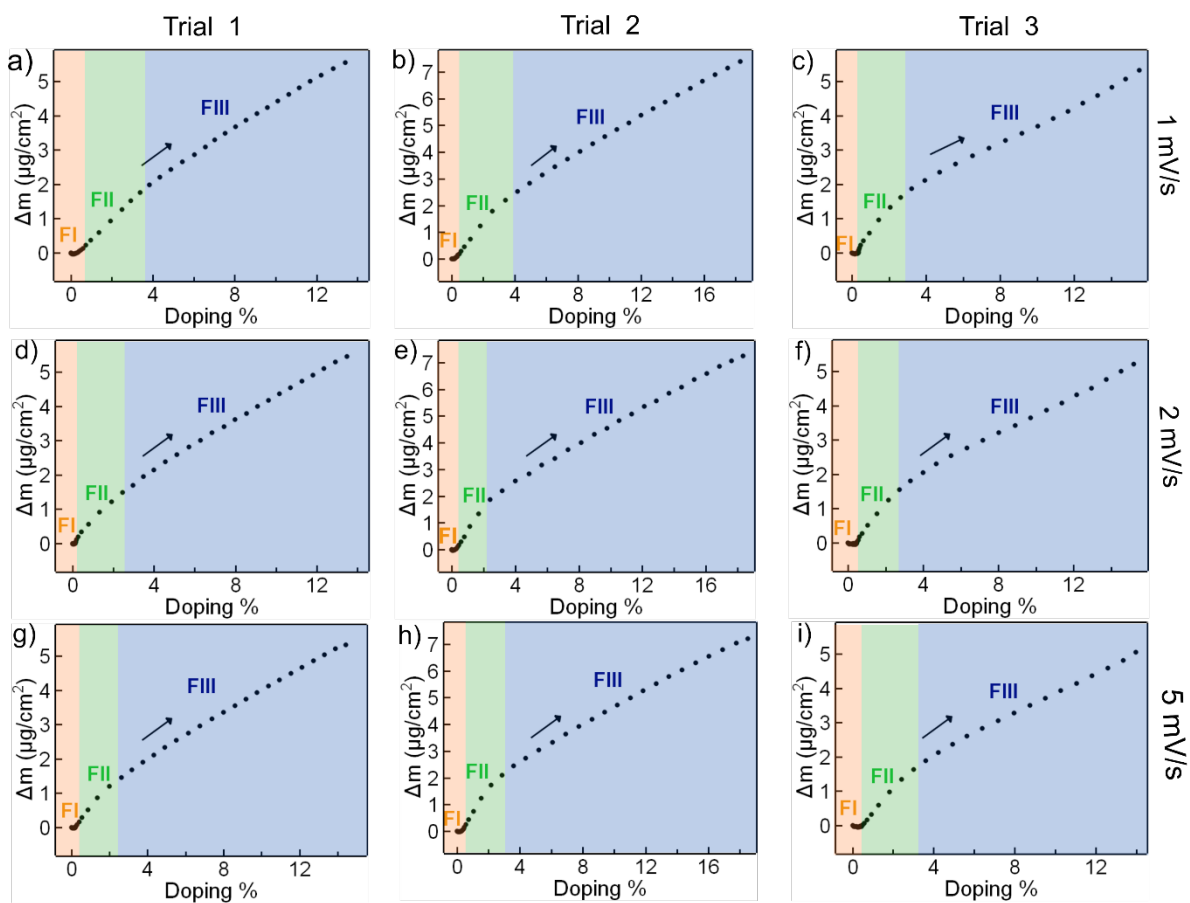


**Figure S9.**  $\Delta m$  vs doping percentage for the scan rates of 1, 2, and 5 mV/s for three separate P3HT films during the CV oxidation cycle with QCM-D.



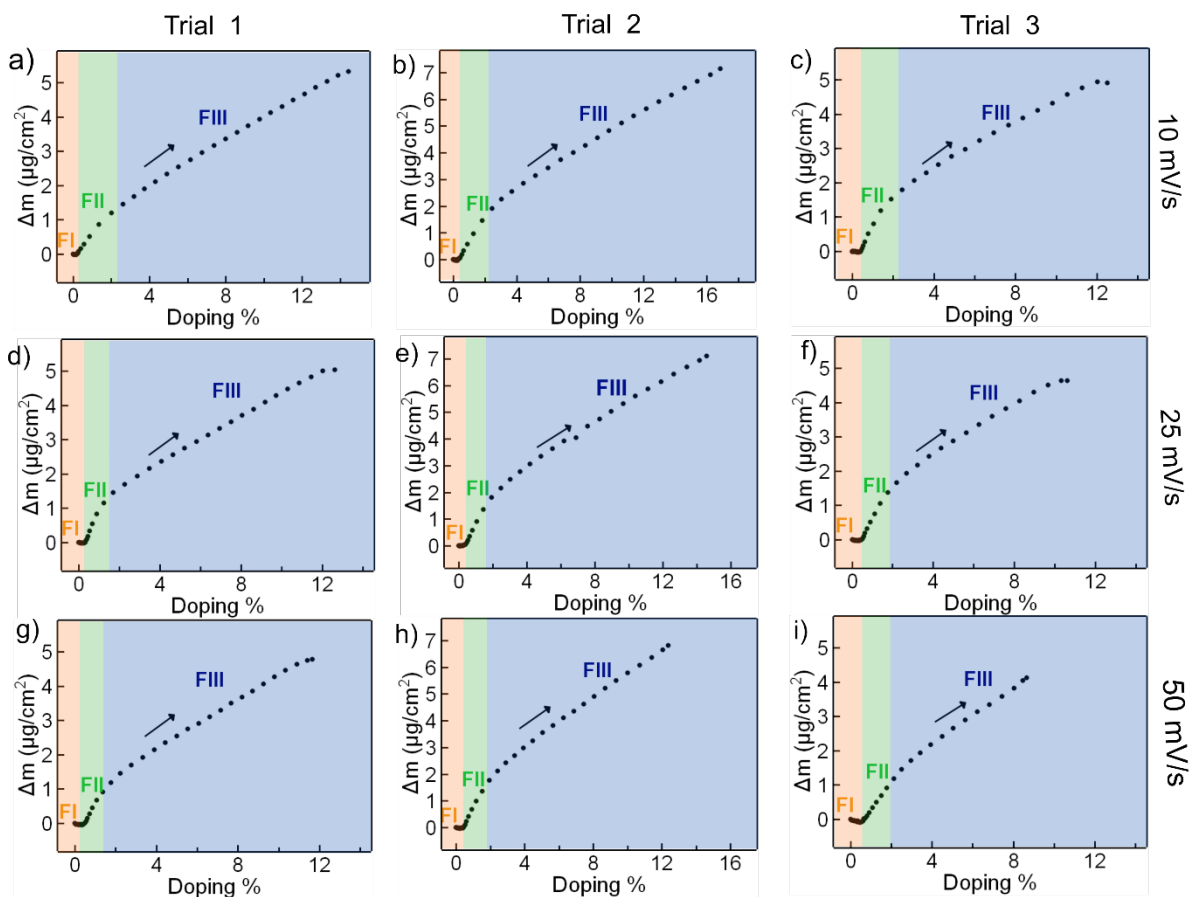


**Figure S10.**  $\Delta m$  vs doping percentage for the scan rates of 10, 25, and 50 mV/s for three separate P3HT films during the CV oxidation cycle with QCM-D.

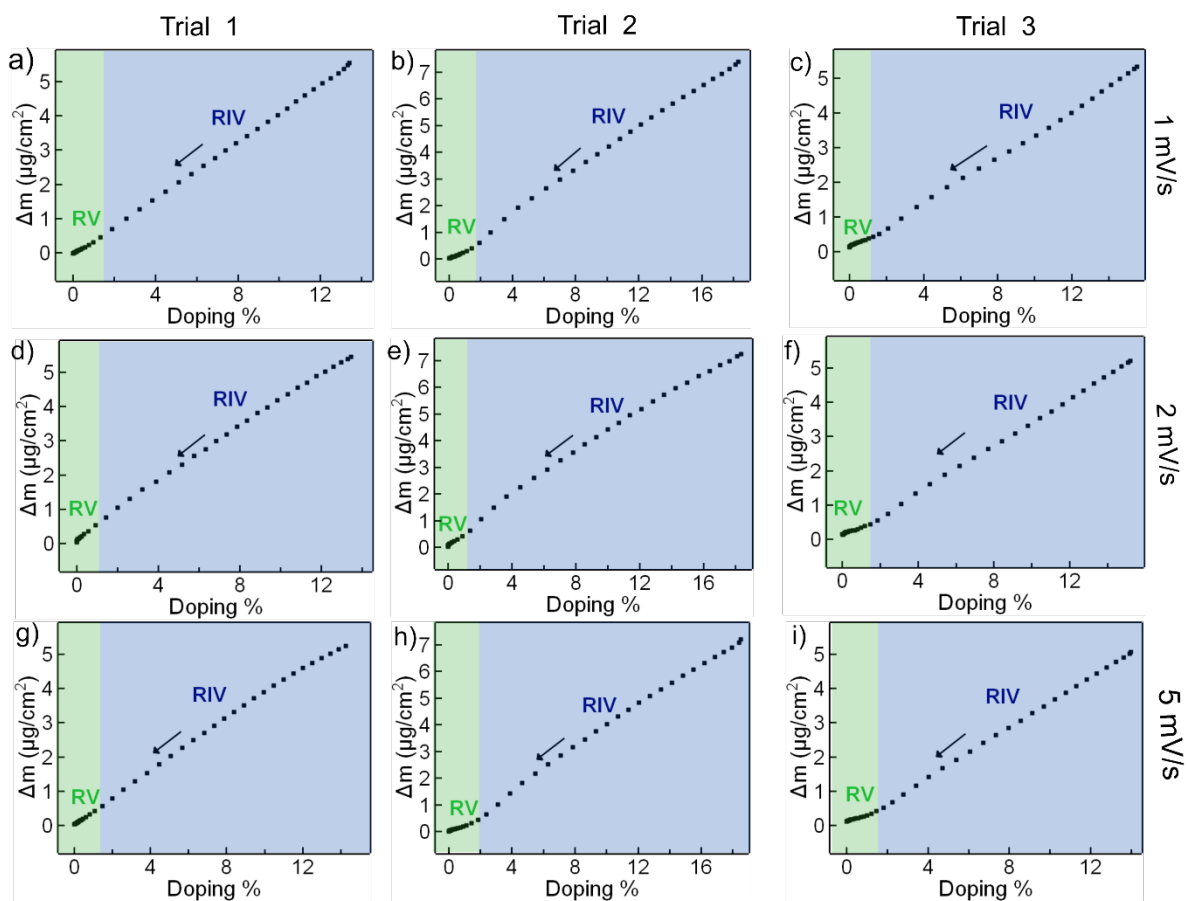


**Figure S11.**  $\Delta m$  vs doping percentage for the scan rates of 1, 2, and 5 mV/s for three separate P3HT films during the CV reduction cycle with QCM-D.

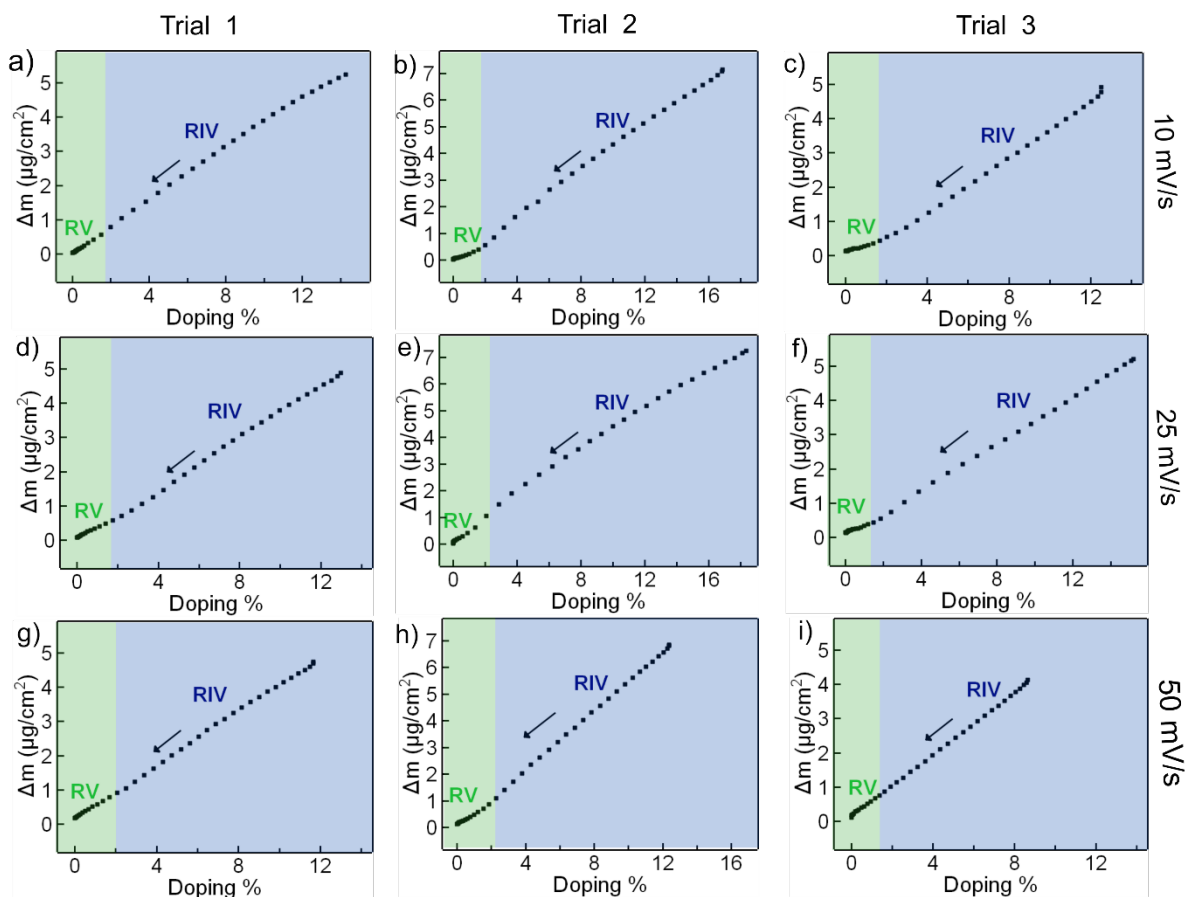


**Figure S12.**  $\Delta m$  vs doping percentage for the scan rates of 10, 25, and 50 mV/s for three separate P3HT films during the CV reduction cycle with QCM-D.

**Table S8.** Summary of the transition doping percentages with varying galvanostatic charge-discharge C-rates. Only oxidation is described because no distinguishable regions were observed for reduction.

	Transition value for Doping regions (%)
C- Rate( $h^{-1}$ )	Oxidation
	FI-FII
5	$3.22 \pm 0.26$
10	$3.47 \pm 0.24$
20	$3.68 \pm 0.32$

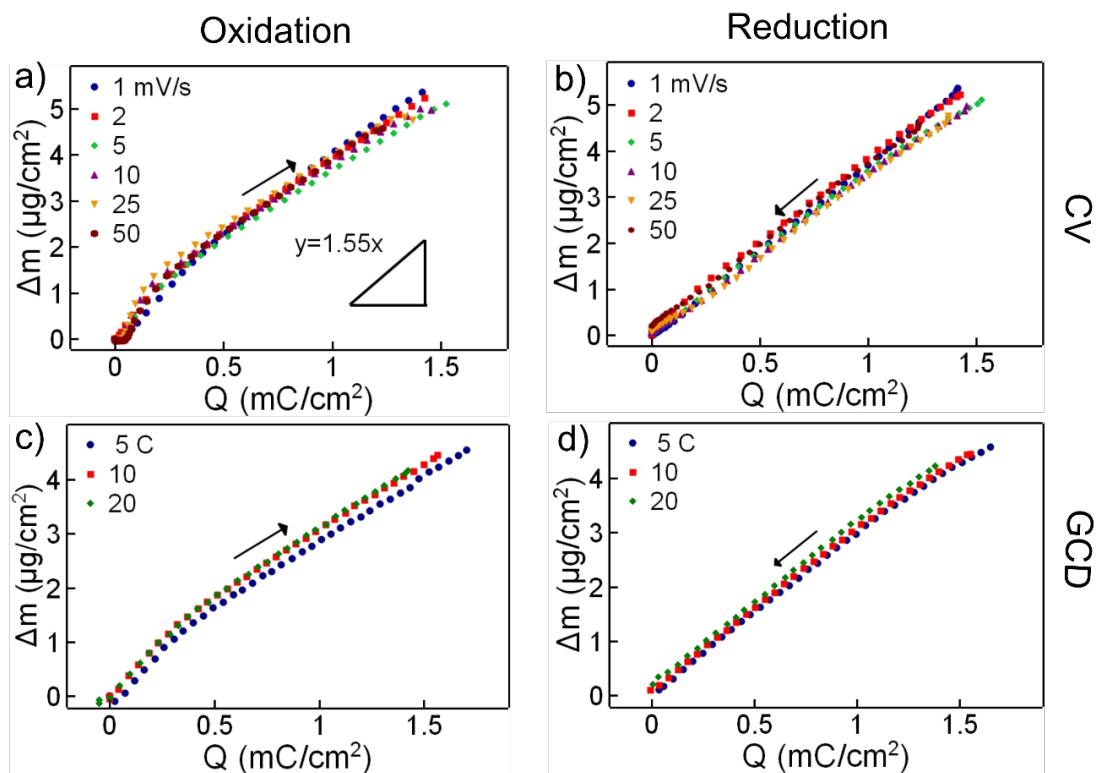


**Figure S13.** Mass change with charge at different scan rates for both a) oxidation and b) reduction in EQCM-D during cyclic voltammetry. Mass change with charge at different C-rates for c) oxidation and d) reduction in EQCM-D with galvanostatic charge-discharge experiments.

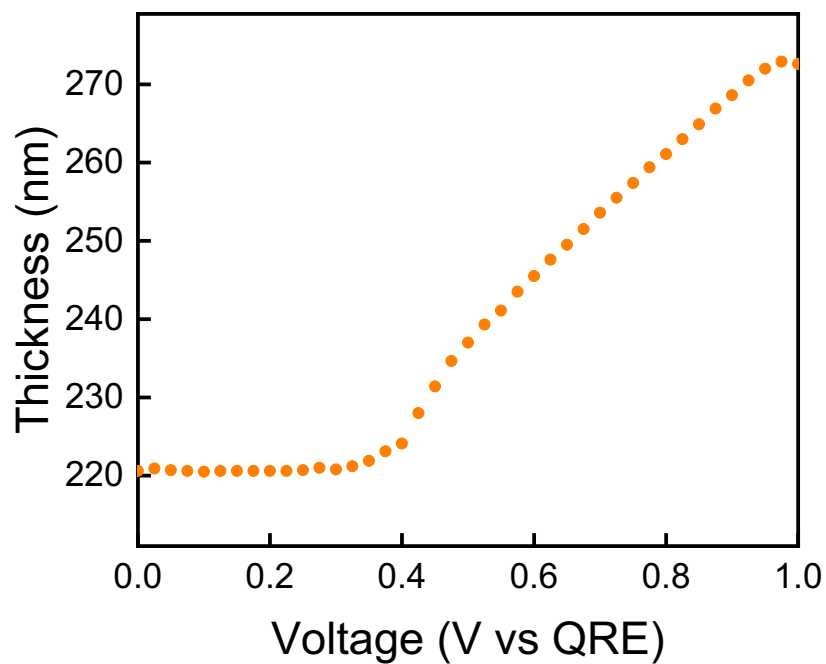


**Figure S14.** P3HT film thickness with increasing voltage at a scan rate of 10 mV/s during oxidation. Thickness was calculated from Sauerbrey equation. The dry film thickness was 215 nm. The electrolyte was 0.5 M lithium triflate in PC.

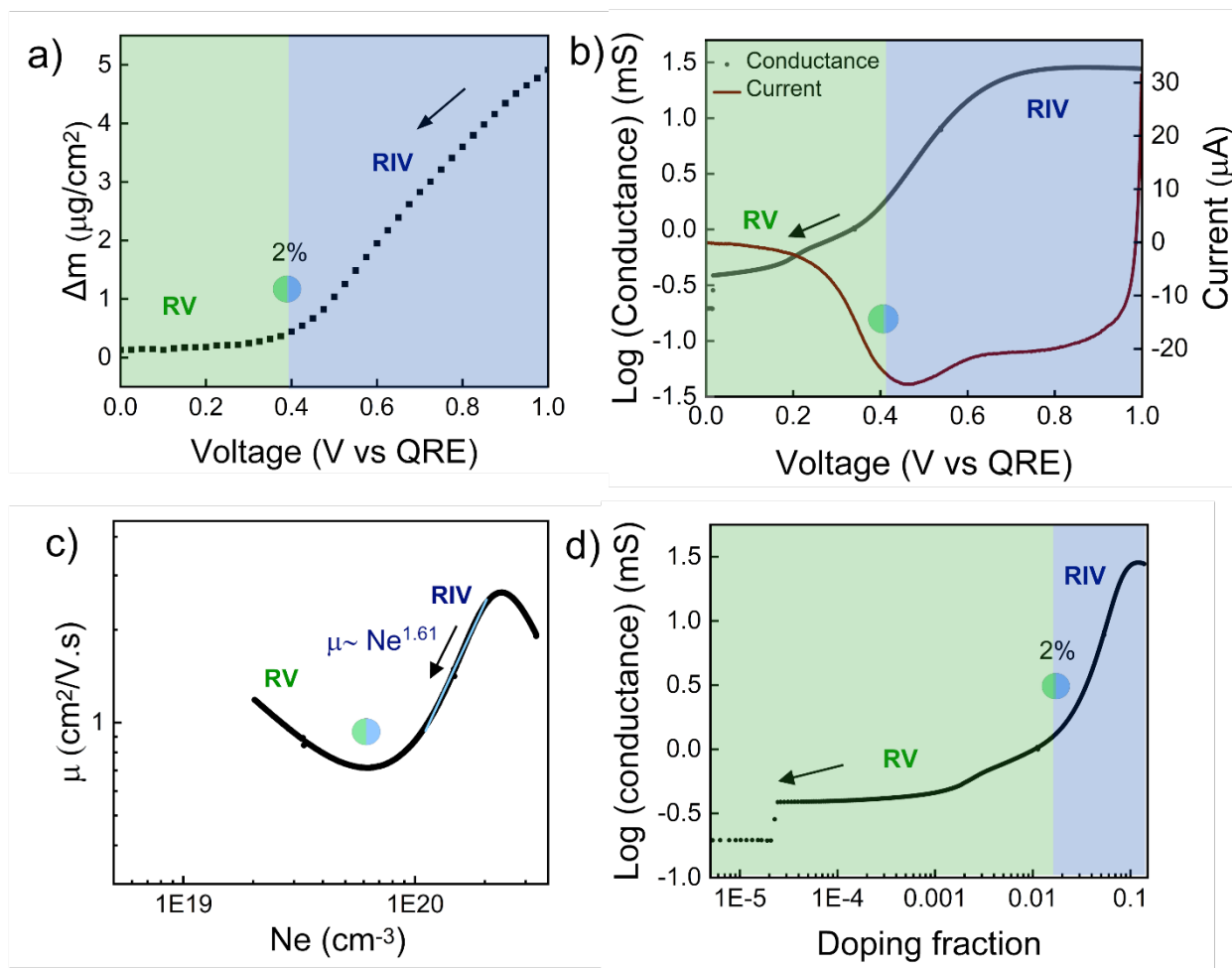


**Figure S15.** a) Mass change with voltage during reduction in EQCM-D with cyclic voltammetry experiments at a scan rate of 10 mV/s. b) Conductance and current change with voltage also at a scan rate of 10 mV/s for reduction cycle. c) Dependence of charge carrier concentration on mobility and d) log (conductance) with log (doping fraction) at a scan rate of 10 mV/s during reduction. The coloured circles separate the different doping regions, as originally described in **Figure 2d** and **Table S1**. The values assigned to the circles represent the transition doping level, as identified in **Figure 2f** and **Table S7**.

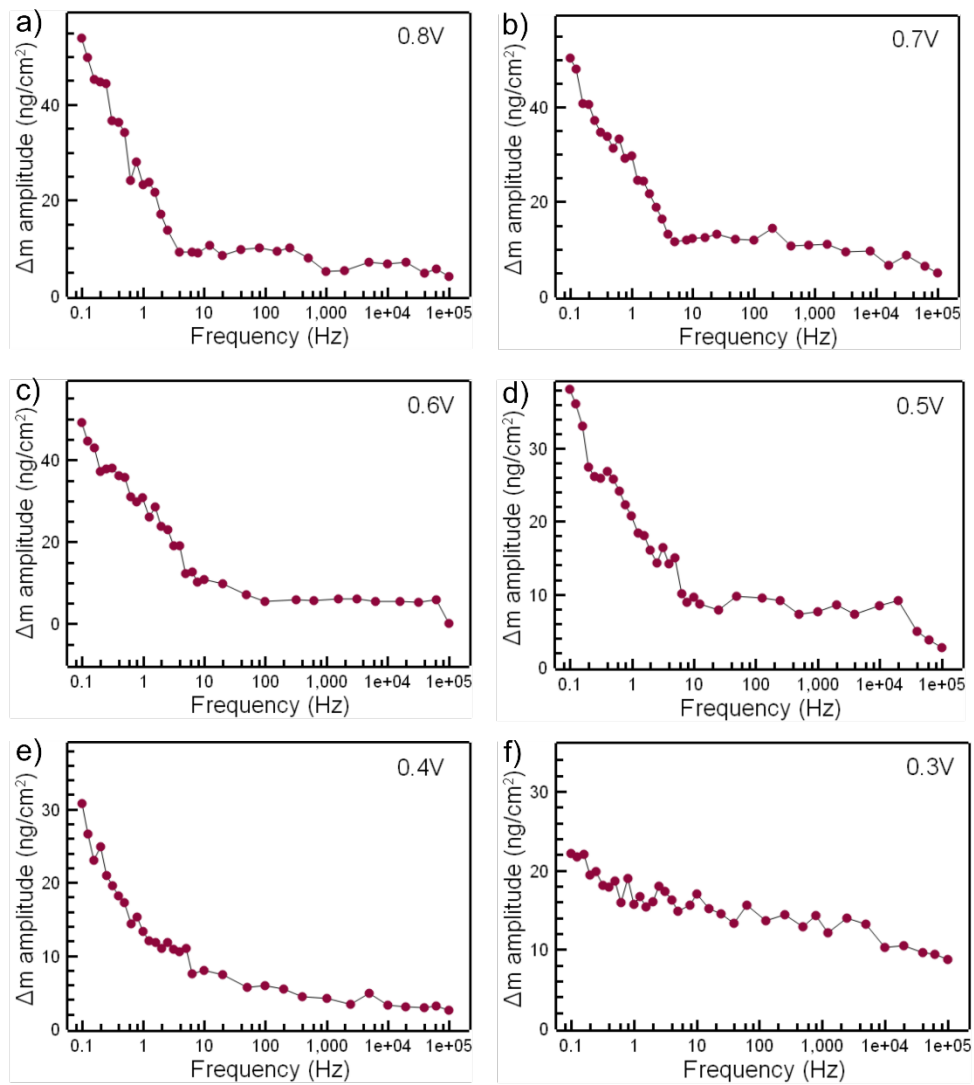


**Figure S16.** Amplitude of the mass response for P3HT during EIS at different applied potentials of a) 0.8 V, b) 0.7 V, c) 0.6 V, d) 0.5 V, e) 0.4 V, and f) 0.3 V vs QRE.



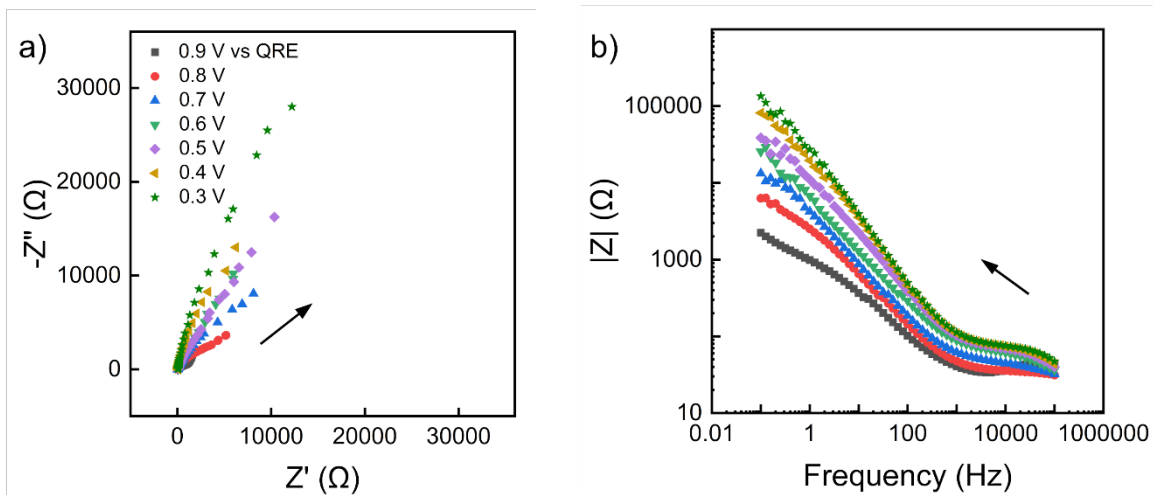


**Figure S17.** a) Nyquist and b) Bode plots for different potential biases. The arrow indicates the direction of decreasing frequency.

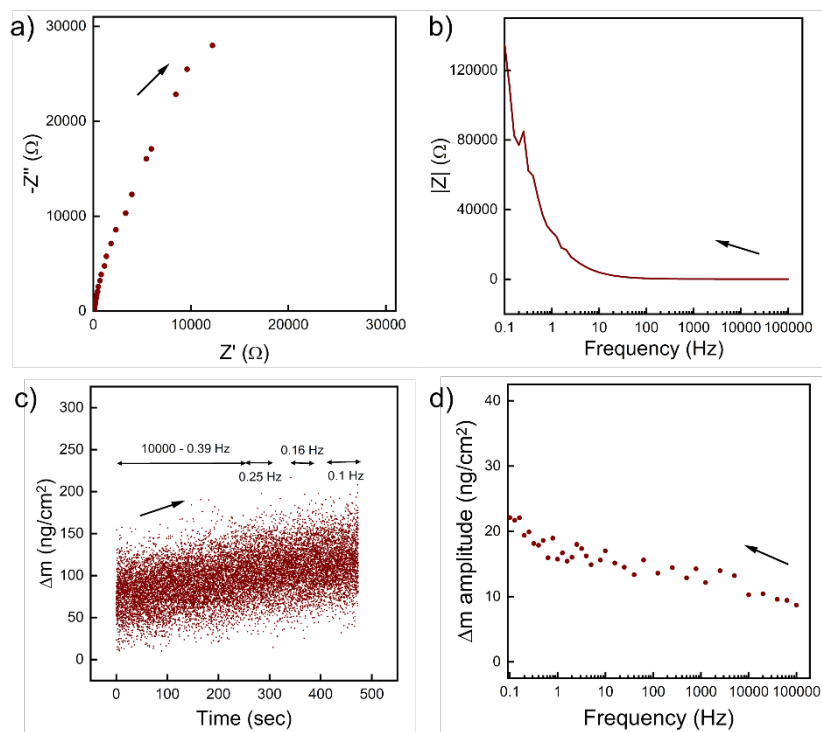


**Figure S18.** a) Nyquist and b) Bode plots, along with the simultaneous c) mass response of P3HT at 0.3 V vs QRE in the same configuration as Fig. 2. d) Amplitude of the mass change vs EIS frequency.

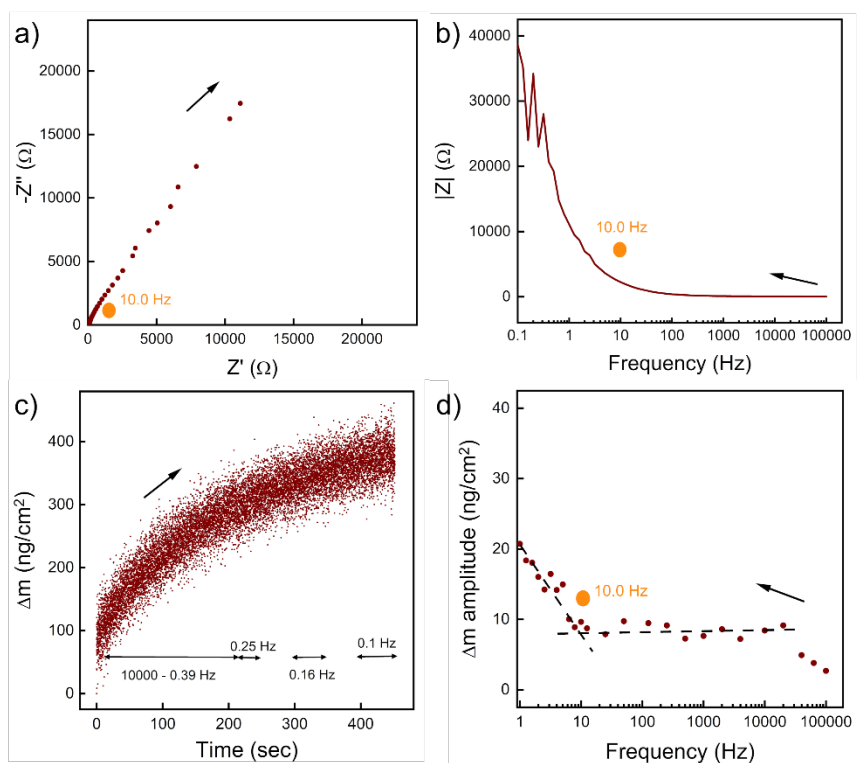


**Figure S19.** a) Nyquist and b) Bode plots, along with the simultaneous c) mass response of P3HT at 0.5 V vs QRE in the same configuration as Fig. 2. d) Amplitude of the mass change vs EIS frequency. The dot denotes the transition frequency for reaction- to diffusion-limited behavior. The arrow denotes the progression of time in the experiment itself.

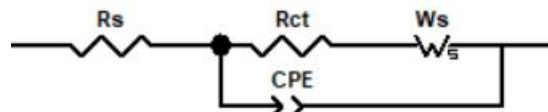


**Figure S20.** Equivalent circuit used to model the EIS data.

- $R_s$  = solution resistance
- $R_{ct}$  = charge transfer resistance
- CPE = Constant phase element
- $W_s$  = Warburg element

The EIS responses were modelled using an equivalent circuit,<sup>1</sup> (**Figure S20**) to examine the solution resistance ( $R_s$ ), charge transfer resistance ( $R_{CT}$ ), constant phase element (CPE), and Warburg element ( $W$ ) characteristics shown in **Table S9**, for each bias applied. With increasing potential, the charge transfer resistance ( $R_{CT}$ ) decreased, likely as a result of the increasing P3HT conductivity. At lower potentials (0.4-0.6V), the Warburg element was not considered in the equivalent circuit. Diffusion coefficients were calculated using the Warburg element for higher potentials (0.7 V – 0.9 V).

**Table S9.** Comparison of onset frequency, diffusion coefficient ( $D$ ), Ohmic resistance ( $R_s$ ), charge transfer resistance ( $R_{CT}$ ), constant phase element (CPE), and Warburg element ( $W_s$ ) characteristics at different potentials from EIS results.<sup>a</sup>

	0.3 V	0.4 V	0.5 V	0.6 V	0.7 V	0.8 V	0.9 V
Onset Frequency of Mass Transport (Hz)	-	11.0	10.0	9.0	4.0	3.0	2.0
$D$ (cm <sup>2</sup> /sec)	-	-	-	-	3.7E-17	2.1E-16	2.7E-15
$R_s$ ( $\Omega$ )	76	74	66	56	44	33	29
$R_{CT}$ ( $\Omega$ )	1.2E+05	5.5E+04	1.8E+04	3.8E+04	1.7E+04	4.0E+03	1.3E+03
CPE-T (F)	6.4E-06	7.6E-06	1.6E-05	4.1E-05	5.3E-05	6.6E-05	1.3E-04
CPE-P	0.88	0.87	0.79	0.71	0.73	0.74	0.69
$W_s$ -R ( $\Omega$ )	-	-	-	-	3.9E+04	2.8E+06	2.3E+05
$W_s$ -T (s)	-	-	-	-	3.9E+00	1.1E+06	1.6E+03
$W_s$ -P	-	-	-	-	0.97	0.48	0.69
$\chi^2$ <sup>a</sup>	0.001	0.0008	0.0005	0.0003	0.0002	0.0003	0.0003

<sup>a</sup>Data from one sample shown here. Three samples were analyzed, and the overall trend remained the same, but the absolute values varied from experiment-to-experiment due to variations in the film thickness.

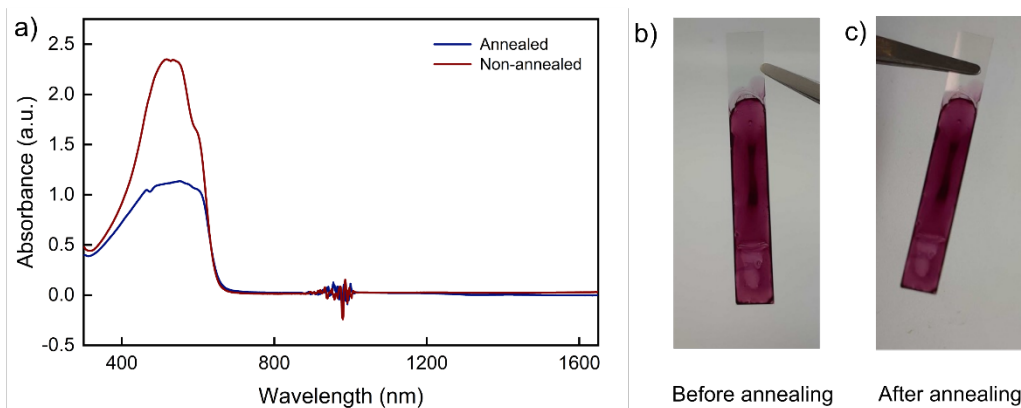


**Figure S21** a) UV-Vis spectra for an annealed (vapor annealing using THF for 12h) and unannealed P3HT film coated on ITO-coated glass and b,c) digital images thereof.

### Sample calculation for determining the doping %

For a scan rate of 10 mV/s, the calculated charge of one sample acquired during oxidation is 1640  $\mu\text{C}$ . Assuming that each electron can be assigned to the doping of one thiophene unit, the percentage of doped thiophene units can be calculated as follows:

$$\text{Moles of electrons transferred} = \frac{\text{Coulombs of charge transferred}}{\text{Faraday's constant}} \quad \text{S1}$$

Therefore,  $1640 \mu\text{C} / 9.65 \times 10^{10} \frac{\mu\text{C}}{\text{mol}} = 1.71 \times 10^{-8}$  moles of electrons transferred, where Faraday constant = 96485 C/mol.

If the mass of the dry P3HT film is  $2.43 \times 10^{-5}$  g (measured using QCM-D) and if the molecular weight of each repeat unit is  $196.35 \frac{\text{g}}{\text{mol}}$ , then the moles of thiophene repeat units in the given film is as  $2.43 \times 10^{-5} \text{ g} / 196.35 \frac{\text{g}}{\text{mol}} = 1.23 \times 10^{-7}$  moles of thiophene repeat units.

The percentage of thiophene units that are doped may be calculated as follows:

$$\text{Doping \%} = \frac{\text{moles of electrons transferred}}{\text{moles of thiophene repeat units}} \times 100\%$$

Therefore,  $1.71 \times 10^{-8}$  mole of electrons /  $1.23 \times 10^{-7}$  moles of thiophene units = 13.77 %. Taken together, 13.77 % of the thiophene units in the given film were doped based upon this sample calculation.

## Calculation for determining charge carrier concentration and mobility

Charge carrier concentration ( $N_e$ ) was calculated from the integrated charge  $Q$  obtained from cyclic voltammetry (see **Figure 2b**). Then, Equation S3 was used to obtain the charge carrier concentration at various doping levels. The real time thickness (see **Figure S16**) was incorporated while calculating the volume of the film.

$$\text{Charge carrier concentration (} N_e \text{)} = \frac{\text{Integrated charge (} Q \text{)} \times \text{Avogadro's number (} N_a \text{)}}{\text{Faraday's constant (} F \text{)} \times \text{Volume (} V \text{)}} \quad (\text{S3})$$

Mobility was calculated from conductance of the film measured on the IDE substrate (see **Figure 7b**). Conductivity ( $\sigma$ ) of the P3HT film was calculated from Equation S4 where the film thickness was assumed to be 215 nm and real time thickness change (see **Figure S16**) was incorporated while calculating conductivity. Mobility ( $\mu$ ) was calculated using Equation S5, where  $e$  is the charge of 1 electron.

$$\text{Conductivity (} \sigma \text{)} = \frac{\text{Conductance (} G \text{)} \times \text{gap width (} W \text{)}}{\text{thickness (} t \text{)} \times \text{IDE length (} L \text{)}} \quad (\text{S4})$$

$$\text{Mobility (} \mu \text{)} = \frac{\text{Conductivity (} \sigma \text{)}}{N_e \times e} \quad (\text{S5})$$

## References

1. Y.-F. Liu, K. Krug and Y.-L. Lee, *Nanoscale*, 2013, **5**, 7936-7941.